

Optimizing the Description of the Delta Region in the Ghent Hybrid Model for Pion Production

Matthias Hooft

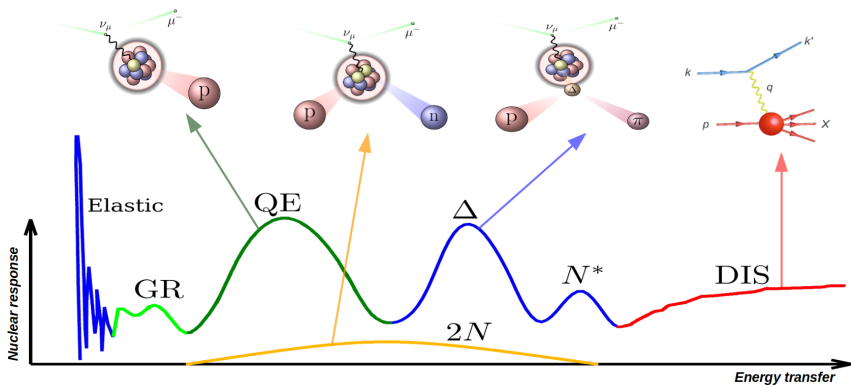
A. Nikolakopoulos, J. García Marcos, T. Franco-Muñoz, R.
González-Jiménez, N. Jachowicz



Single Pion Production

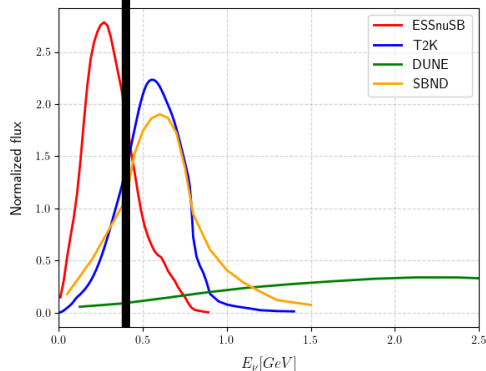
Single pion production (SPP):

- Electron or neutrino interacts with a nucleon in the nucleus and creates a pion
- Mostly excitation to a resonance



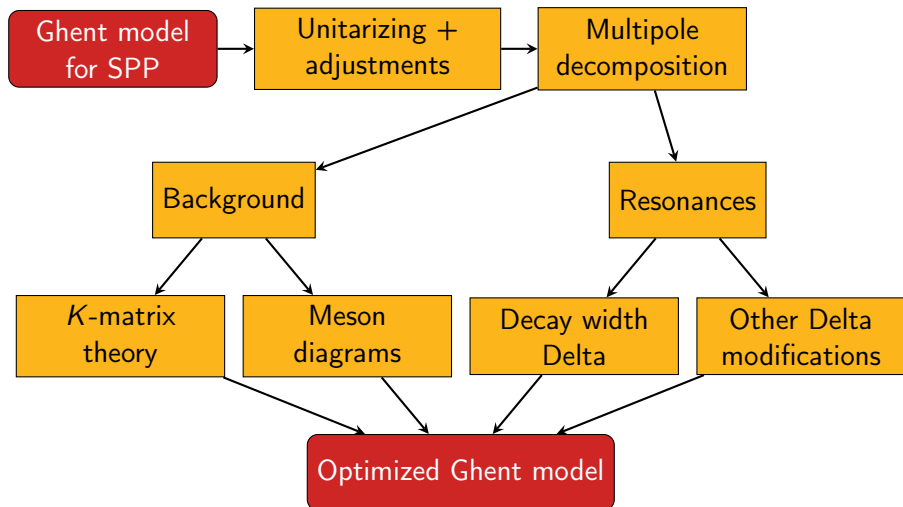
Why Pions?

SINGLE-PION PRODUCTION THRESHOLD



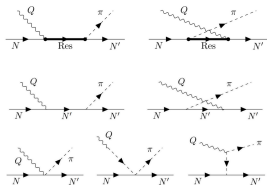
- For T2K, HK and SBND: SPP 20% of total interaction rate
- SPP important non-resonant background for 0π
- Modeling SPP is crucial for ν -energy reconstruction

What we did



Ghent model for SPP

Ghent model
for SPP



**TREE-LEVEL
DIAGRAMS**

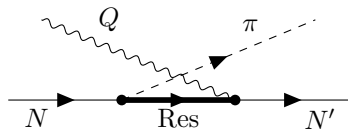
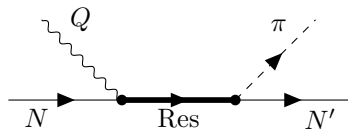
LOW ENERGY

HIGH ENERGY

Ghent model for SPP

Low-energy model:

- Resonant part: s - and u -channel diagrams of $P_{33}(1232)$, $P_{11}(1430)$, $D_{13}(1520)$ and $S_{11}(1535)$

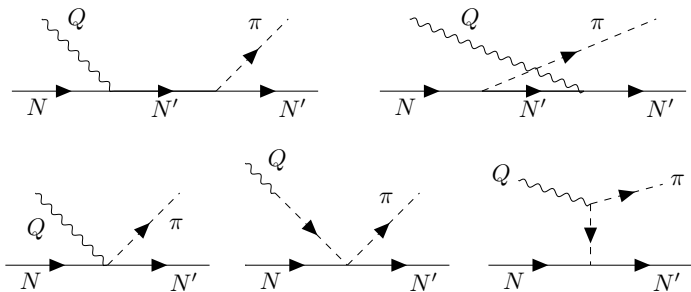


Ghent Model for SPP

Ghent model for SPP

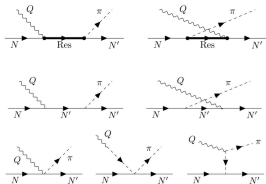
Low-energy model:

- Resonant part: s - and u -channel diagrams of $P_{33}(1232)$, $P_{11}(1430)$, $D_{13}(1520)$ and $S_{11}(1535)$
- Background part: lowest order terms in HNV-Lagrangian (Details: Phys. Rev. D 76, 033005 (2007).)



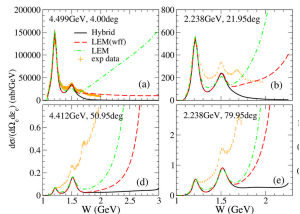
Ghent model for SPP

Ghent model
for SPP



**TREE-LEVEL
DIAGRAMS**

LOW ENERGY

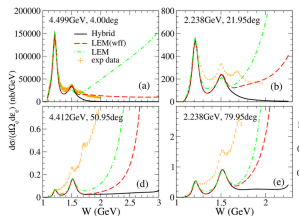
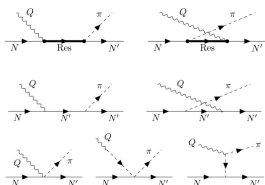


REGGE THEORY

HIGH ENERGY

Ghent model for SPP

Ghent model
for SPP



**TREE-LEVEL
DIAGRAMS**



**HYBRID
MODEL**



REGGE THEORY

LOW ENERGY

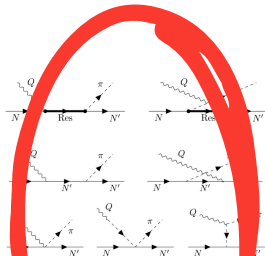


HIGH ENERGY

More details: Phys.Rev.D 95 (2017) 11, 113007

Ghent model for SPP

Ghent model
for SPP



**WE FOCUS
ON LOW ENERGY
MODEL**

**TREE-LEVEL
DIAGRAMS**

**HYBRID
MODEL**

← REGGE THEORY

LOW ENERGY

HIGH ENERGY

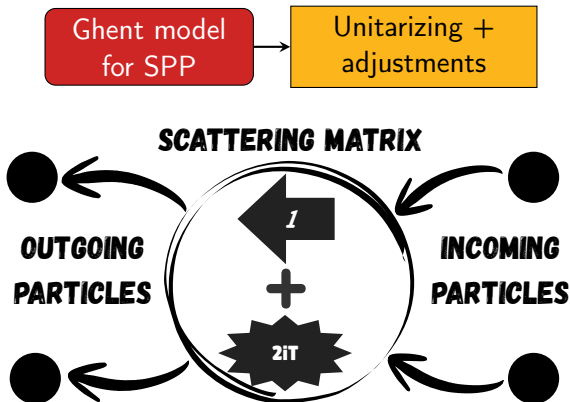
Improvements



Key goals of this work:

- Focus on Delta region
- Add more physics to the model, as much as possible!
- Use as many physics constraints as possible to minimize the number of parameters in the model

Improvements



- Scattering matrix S transforms incoming state $|I\rangle$ into final state $|F\rangle$.
- Scattering matrix $S = \mathbb{I} + 2iT$.
- Scattering amplitude $T_{IF} = \langle F | T | I \rangle$.

Improvements

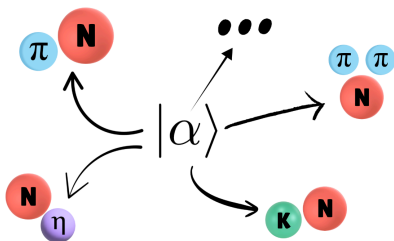


Unitarity: probability of all possible transitions is 1 $\Rightarrow SS^\dagger = \mathbb{I}$.

$S = \mathbb{I} + 2iT$ and invariance under time reversal:

$$\sum_{\alpha} \langle \alpha | T_{J,L,S,I} | F \rangle^* \langle \alpha | T_{J,L,S,I} | I \rangle \in \mathbb{R} \quad (1)$$

$|\alpha\rangle$: all possible intermediate states with given invariant mass W .

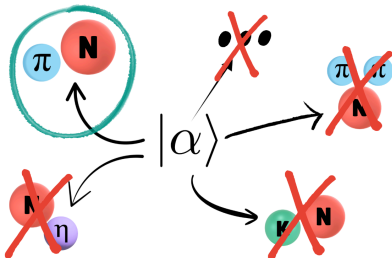


Improvements

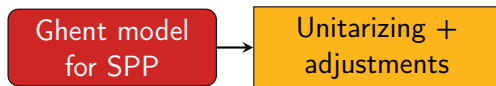


$$\sum_{\alpha} \langle \alpha | T_{J,L,S,I} | F \rangle^* \langle \alpha | T_{J,L,S,I} | I \rangle \in \mathbb{R} \quad (2)$$

Energy below 2-pion production threshold: only $\alpha =$ pion-nucleon state is possible



Improvements



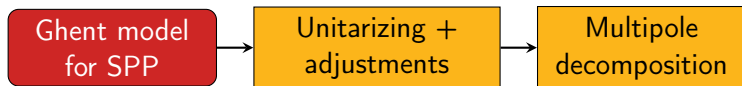
Watson's theorem allows one to impose unitarity constraints by fixing the phase of the pion production amplitude:

- Below 2-pion production threshold
- Initial state = $\gamma/W^\pm/Z + N$
- Final states = $\pi + N$

$$\langle N\pi | T_{J,L,S,I} | N\pi \rangle^* \langle N\pi | T_{J,L,S,I} | N, \gamma/W^\pm/Z \rangle \in \mathbb{R} \quad (3)$$

\Rightarrow More physics: phase of single pion-production amplitude = phase of pion-nucleon scattering amplitude with same quantum numbers

Multipole Decomposition



Unitarity constraints for each amplitude with fixed angular momenta J, L, S and isospin I

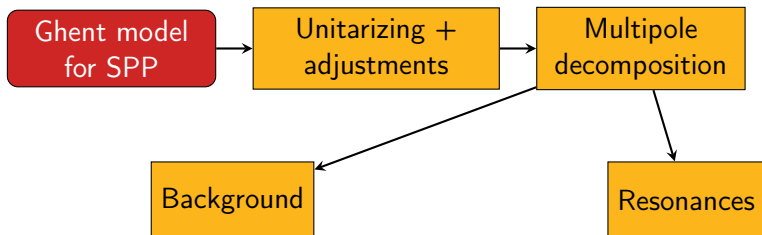
$$\langle N\pi | T_{J,L,S,I} | N\pi \rangle^* \langle N\pi | T_{J,L,S,I} | N, \gamma/W^\pm/Z \rangle \in \mathbb{R} \quad (4)$$

Implementing these constraints requires:

- Expansion of scattering amplitudes $\langle F | T | I \rangle$ in multipoles $E_{I\pm}, M_{I\pm}, S_{I\pm}$
- Unitarize each multipole separately

For more details: A. Berends, A. Donnachie and D.L. Weaver, Nucl.Phys.B 4 (1967) 1-53

Background and Resonances



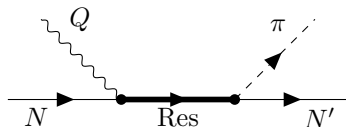
Implementing unitarity constraints

$$\langle N\pi | T_{J,L,S,I} | N\pi \rangle^* \langle N\pi | T_{J,L,S,I} | N, \gamma/W^\pm/Z \rangle \in \mathbb{R} \quad (5)$$

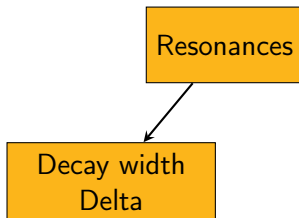
Split total scattering T -matrix: $T = T_{BG} + T_{Res}$.

Resonances

- Δ -resonance ($P_{33}(1232)$)
- $P_{11}(1430)$, $D_{13}(1520)$ and $S_{11}(1535)$ (untouched in this work)



Decay Width Delta



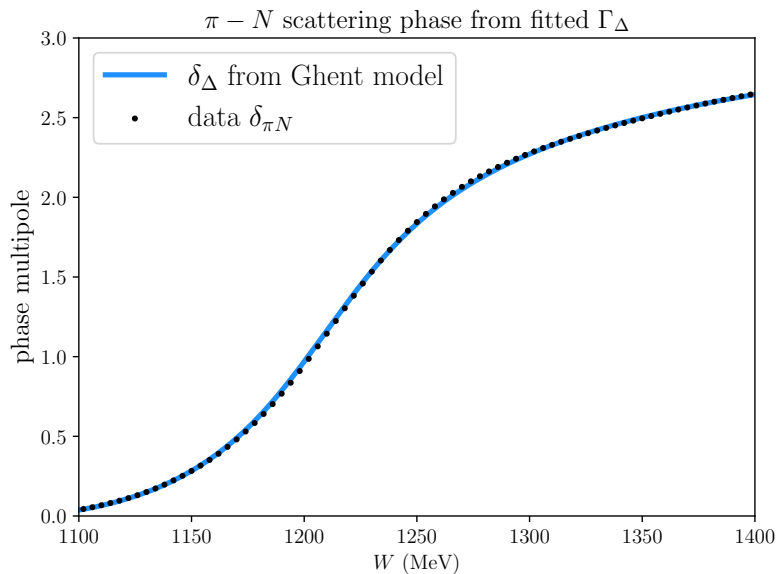
Multipoles with contribution from Delta resonance: $T_{Res} \gg T_{BG}$

$$T_{res} = \langle F | \frac{A_{\Delta} e^{i\phi_{\Delta}}}{W^2 - M_{\Delta}^2 + iM_{\Delta}\Gamma_{\Delta}(W)} | I \rangle \quad (6)$$

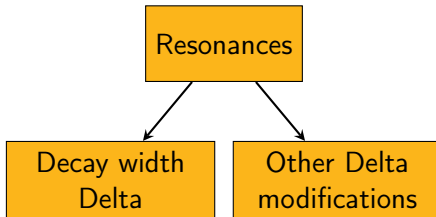
Implementing unitarity constraints:

- Phase $\phi_{\Delta} = 0$ (less parameters)
- Decay width $\Gamma_{\Delta} = \frac{M_{\Delta}^2 - W^2}{M_{\Delta}} \tan(\delta_{\pi N}(W))$ with $\delta_{\pi N}$ from a fit to data

Decay Width Delta



Other Modifications Delta

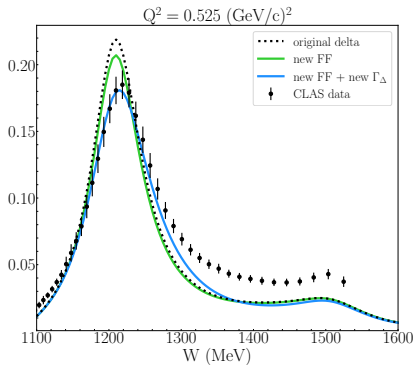
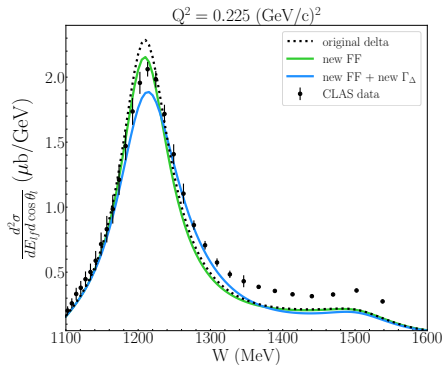


Additional modifications:

- Rarita-Schwinger theory: spurious $J = \frac{1}{2}$ contributions put to zero
- Form factors obtained from MAID fits (Phys.Rev.D 107 (2023) 5, 053007)



Results Resonances

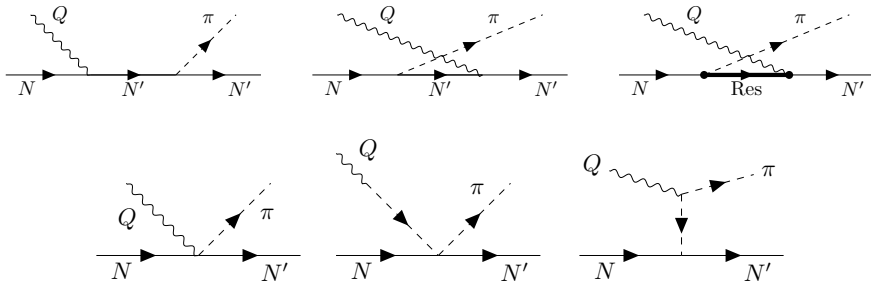


- Changing form factors: reduction of the height of the delta peak
- Changing decay width: peak decreases even further and small shift toward higher energies

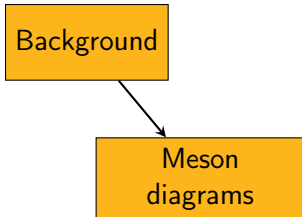
Background

Background contains:

- HNV-diagrams
- u -channel diagrams cross resonances (pole far away from SPP energies)
- Extra meson diagrams

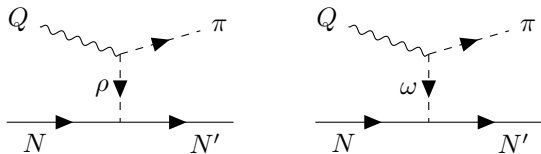


Meson Exchange Diagrams

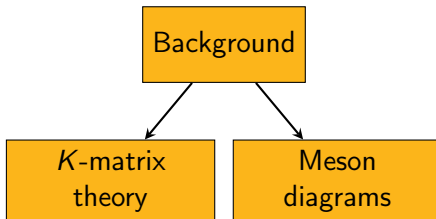


Added ρ - and ω -exchange diagrams:

- Widely used Lagrangian: Nucl. Phys. A 627, 645 (1997)
- Couplings and form factors from MAID model



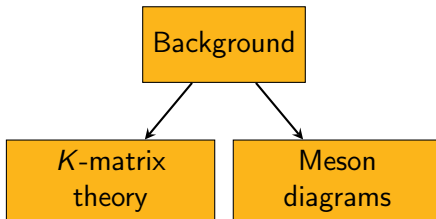
Unitarizing the Background



Invariant mass below two-pion production threshold:

$$\mathbf{T} = \begin{bmatrix} \mathbf{T}_{\gamma\gamma} & \mathbf{T}_{\gamma\pi} \\ \mathbf{T}_{\gamma\pi} & \mathbf{T}_{\pi\pi} \end{bmatrix}$$

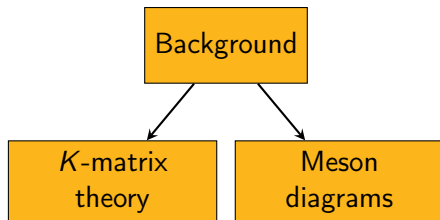
Unitarizing the Background



Invariant mass below two-pion production threshold:

$$\mathbf{T} = \begin{bmatrix} \mathbf{T}_{\gamma\gamma} & \mathbf{T}_{\gamma\pi} \\ \mathbf{T}_{\gamma\pi} & \mathbf{T}_{\pi\pi} \end{bmatrix}$$

The diagram illustrates the unitarization of the transition matrix \mathbf{T} for the process $\gamma + N \rightarrow \gamma + N$ (blue text) and $\gamma + N \rightarrow \pi + N$ (red text). The matrix elements are $\mathbf{T}_{\gamma\gamma}$, $\mathbf{T}_{\gamma\pi}$, and $\mathbf{T}_{\pi\pi}$. The $\mathbf{T}_{\gamma\pi}$ elements are circled in red, and the $\mathbf{T}_{\pi\pi}$ element is circled in green. Arrows indicate the flow of unitarization: a blue arrow points from the $\mathbf{T}_{\gamma\gamma}$ element to the $\gamma + N \rightarrow \gamma + N$ process, a red arrow points from the $\mathbf{T}_{\gamma\pi}$ elements to the $\gamma + N \rightarrow \pi + N$ process, and a green arrow points from the $\mathbf{T}_{\pi\pi}$ element to the $\pi + N \rightarrow \pi + N$ process.

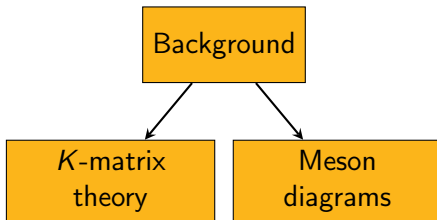


Using Unitarity of S and time reversal invariance \Rightarrow define the K -matrix:

$$T = K + iKT \quad (7)$$

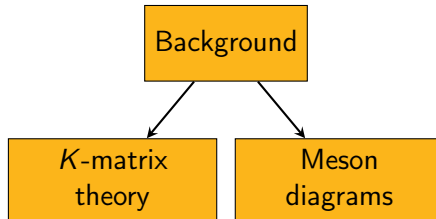
- Scattering K -matrix is real and symmetric
- Our background amplitudes = matrix elements of K -matrix

K-Matrix Theory



$$\begin{bmatrix} \mathbf{T}_{\gamma\gamma} & \mathbf{T}_{\gamma\pi} \\ \mathbf{T}_{\gamma\pi} & \mathbf{T}_{\pi\pi} \end{bmatrix} = \begin{bmatrix} \mathbf{K}_{\gamma\gamma} & \mathbf{K}_{\gamma\pi} \\ \mathbf{K}_{\gamma\pi} & \mathbf{K}_{\pi\pi} \end{bmatrix} + i \begin{bmatrix} \mathbf{K}_{\gamma\gamma} & \mathbf{K}_{\gamma\pi} \\ \mathbf{K}_{\gamma\pi} & \mathbf{K}_{\pi\pi} \end{bmatrix} \begin{bmatrix} \mathbf{T}_{\gamma\gamma} & \mathbf{T}_{\gamma\pi} \\ \mathbf{T}_{\gamma\pi} & \mathbf{T}_{\pi\pi} \end{bmatrix}$$

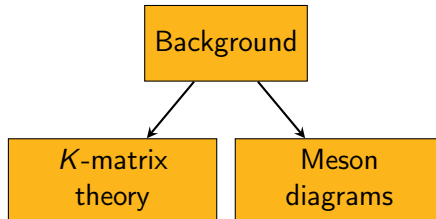
K-Matrix Theory



Neglect the amplitudes proportional to square of EM coupling

$$\begin{bmatrix} \cancel{T}_{\gamma\gamma} & T_{\gamma\pi} \\ T_{\gamma\pi} & T_{\pi\pi} \end{bmatrix} = \begin{bmatrix} \cancel{K}_{\gamma\gamma} & K_{\gamma\pi} \\ K_{\gamma\pi} & K_{\pi\pi} \end{bmatrix} + i \begin{bmatrix} \cancel{K}_{\gamma\gamma} & K_{\gamma\pi} \\ K_{\gamma\pi} & K_{\pi\pi} \end{bmatrix} \begin{bmatrix} \cancel{T}_{\gamma\gamma} & T_{\gamma\pi} \\ T_{\gamma\pi} & T_{\pi\pi} \end{bmatrix}$$

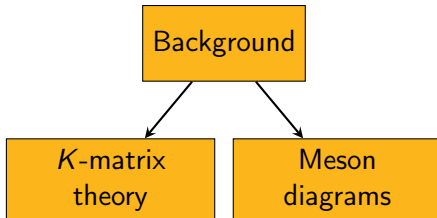
K-Matrix Theory



Combine these elements

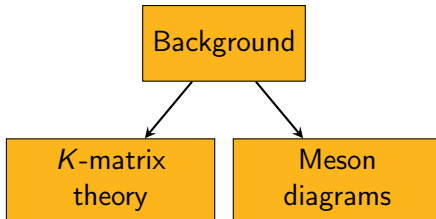
$$\begin{bmatrix} \cancel{T}_{\gamma\gamma} & T_{\gamma\pi} \\ T_{\gamma\pi} & T_{\pi\pi} \end{bmatrix} = \begin{bmatrix} \cancel{K}_{\gamma\gamma} & K_{\gamma\pi} \\ K_{\gamma\pi} & K_{\pi\pi} \end{bmatrix} + i \begin{bmatrix} \cancel{K}_{\gamma\gamma} & K_{\gamma\pi} \\ K_{\gamma\pi} & K_{\pi\pi} \end{bmatrix} \begin{bmatrix} \cancel{T}_{\gamma\pi} & T_{\gamma\pi} \\ T_{\gamma\pi} & T_{\pi\pi} \end{bmatrix}$$

K-Matrix Theory



$$\mathbf{T}_{\gamma\pi} \equiv \mathbf{K}_{\gamma\pi} (1 + i \mathbf{T}_{\pi\pi})$$

K-Matrix Theory



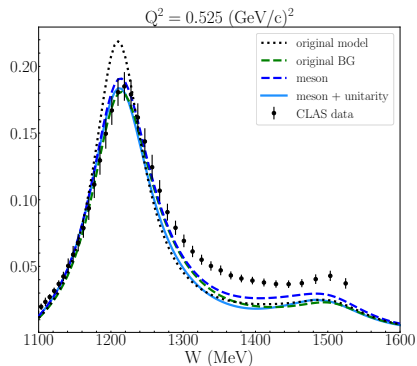
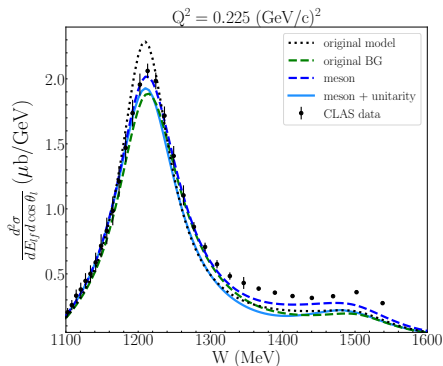
OUR BACKGROUND AMPLITUDES

$$\mathbf{T}_{\gamma\pi} = \mathbf{K}_{\gamma\pi} (1 + i \mathbf{T}_{\pi\pi})$$

UNITARIZED \mathbf{T}_{BG}

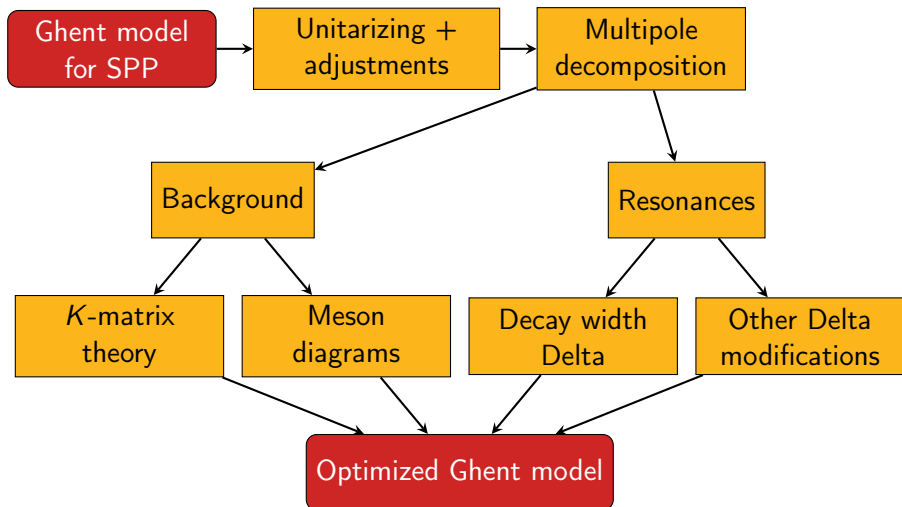
FROM PION-NUCLEON SCATTERING DATA

Background Results

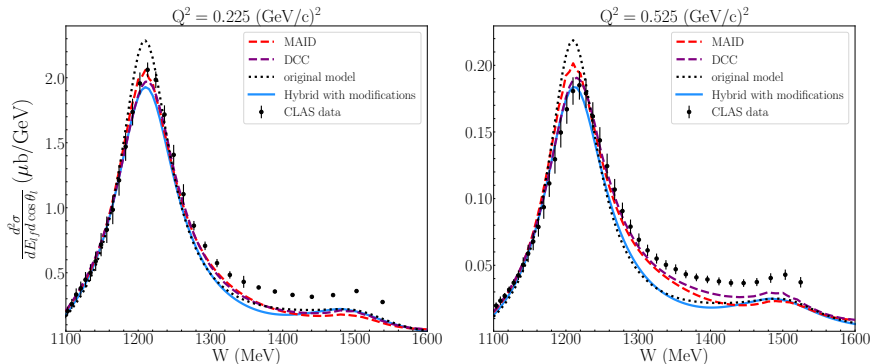


- Adding meson diagrams \Rightarrow Global increase
- Unitarization has limited effect

Results

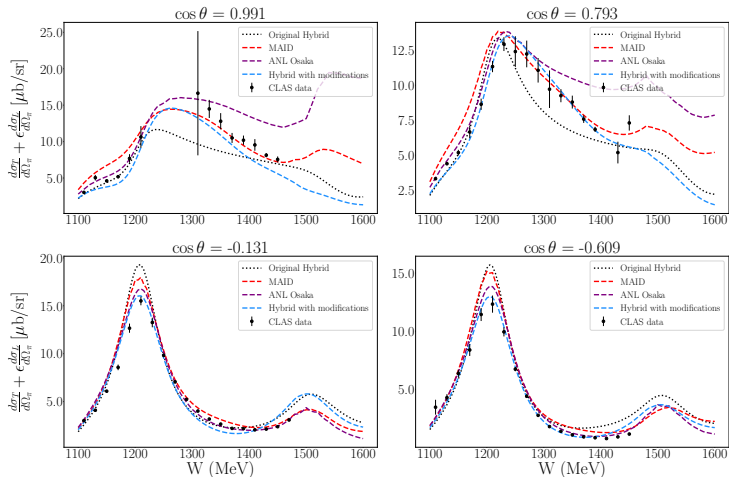


Inclusive Cross Sections



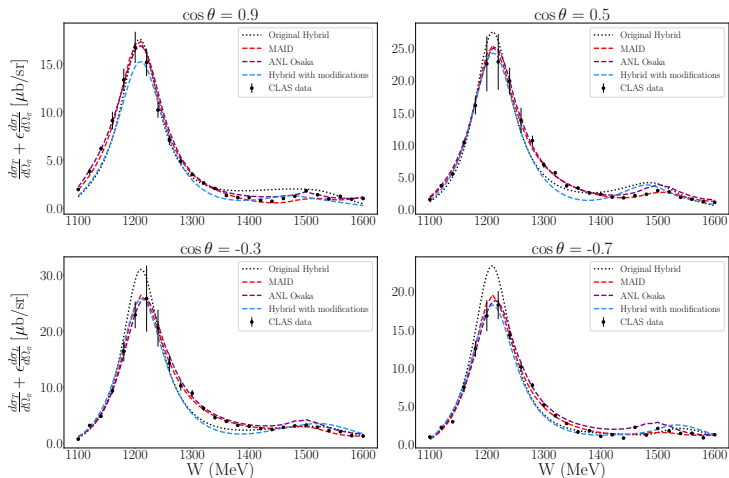
- Delta peak decreases \rightarrow much better agreement with data
- High energy tail almost the same and drops too fast \rightarrow 2-pion production

Exclusive Cross Sections $e + p \rightarrow e + n + \pi^+$



- Prediction for the Delta-peak improved significantly
- High energy tail predictions still need some work

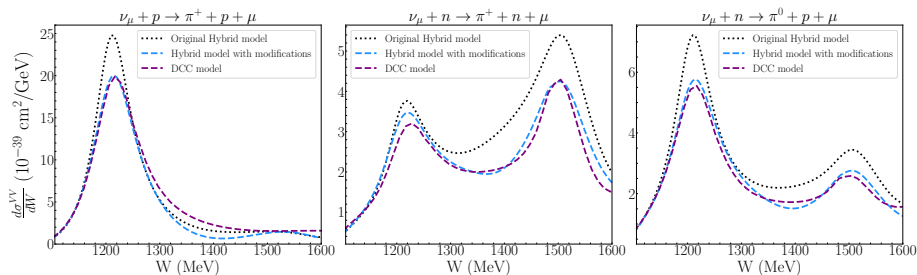
Exclusive Cross Sections $e + p \rightarrow e + p + \pi^0$



- For most angles: prediction for the Delta-peak improved significantly
- High energy tail tends to decrease too fast
- Second resonance region predictions are good

Charged Current SPP:

Vector part of Charged Current SPP compared with DCC model



- Vector part of CC SPP decreases everywhere
- Predictions in good agreement with the DCC model

Conclusion and Outlook

Conclusion:

- Implemented Watson's theorem till 2-pion production threshold
- Improves Delta-peak region for both inclusive and exclusive results for different pion production channels
- Vector part charged current SPP changes significantly

Work for the future:

- Multipole decomposition of axial part (work in progress)
- Put model in the nucleus (work in progress)
- Produce results for neutrinos
- Push model to higher energies: bigger T -matrix and more resonances

Thanks for Listening
Questions?

back up slides

How to get multipoles

Projecting on states with fixed angular momentum J :

$$\langle \lambda_F | T_r^J | \lambda_I \rangle = \int d\Omega_F \langle \Omega_F, \lambda_F | T | \Omega_I, \lambda_I \rangle D_{\lambda_I, \lambda_F}^J(\Omega_F), \quad (8)$$

where:

- $\langle \lambda_F | T_r^J | \lambda_I \rangle = \langle J, M, \lambda_F | T_r^J | J, M, \lambda_I \rangle$
- Helicity initial nucleon = λ_I , helicity outgoing nucleon = λ_F , helicity photon = r

How to get multipoles

Relations between J -projected helicity amplitudes and multipoles:

$$E_{l+}^V = \frac{\sqrt{2}}{4i(l+1)} \left(\sqrt{\frac{l}{l+2}} \left(-\left\langle \frac{1}{2} \left| T_{r=-1}^J \right| \frac{3}{2} \right\rangle - \left\langle -\frac{1}{2} \left| T_{r=-1}^J \right| \frac{3}{2} \right\rangle \right) + \left\langle \frac{1}{2} \left| T_{r=-1}^J \right| \frac{1}{2} \right\rangle + \left\langle -\frac{1}{2} \left| T_{r=-1}^J \right| \frac{1}{2} \right\rangle \right),$$

$$E_{(l+1)-}^V = \frac{\sqrt{2}}{4i(l+1)} \left(\sqrt{\frac{l+2}{l}} \left(\left\langle \frac{1}{2} \left| T_{r=-1}^J \right| \frac{3}{2} \right\rangle - \left\langle -\frac{1}{2} \left| T_{r=-1}^J \right| \frac{3}{2} \right\rangle \right) + \left\langle \frac{1}{2} \left| T_{r=-1}^J \right| \frac{1}{2} \right\rangle - \left\langle -\frac{1}{2} \left| T_{r=-1}^J \right| \frac{1}{2} \right\rangle \right),$$

$$M_{l+}^V = \frac{\sqrt{2}}{4i(l+1)} \left(\sqrt{\frac{l+2}{l}} \left(\left\langle \frac{1}{2} \left| T_{r=-1}^J \right| \frac{3}{2} \right\rangle + \left\langle -\frac{1}{2} \left| T_{r=-1}^J \right| \frac{3}{2} \right\rangle \right) + \left\langle \frac{1}{2} \left| T_{r=-1}^J \right| \frac{1}{2} \right\rangle + \left\langle -\frac{1}{2} \left| T_{r=-1}^J \right| \frac{1}{2} \right\rangle \right),$$

$$M_{(l+1)-}^V = \frac{\sqrt{2}}{4i(l+1)} \left(\sqrt{\frac{l}{l+2}} \left(\left\langle \frac{1}{2} \left| T_{r=-1}^J \right| \frac{3}{2} \right\rangle - \left\langle -\frac{1}{2} \left| T_{r=-1}^J \right| \frac{3}{2} \right\rangle \right) - \left\langle \frac{1}{2} \left| T_{r=-1}^J \right| \frac{1}{2} \right\rangle + \left\langle -\frac{1}{2} \left| T_{r=-1}^J \right| \frac{1}{2} \right\rangle \right),$$

$$S_{l+}^V = \frac{q}{2i(l+1)\sqrt{Q^2}} \left(\left\langle \frac{1}{2} \left| T_{r=0}^J \right| \frac{1}{2} \right\rangle + \left\langle -\frac{1}{2} \left| T_{r=0}^J \right| \frac{1}{2} \right\rangle \right),$$

$$S_{(l+1)-}^V = \frac{q}{2i(l+1)\sqrt{Q^2}} \left(\left\langle \frac{1}{2} \left| T_{r=0}^J \right| \frac{1}{2} \right\rangle - \left\langle -\frac{1}{2} \left| T_{r=0}^J \right| \frac{1}{2} \right\rangle \right),$$

Cross Section and Multipole Decomposition

For $e + N \rightarrow e + N' + \pi$ and after integrating over ϕ_π

$$\frac{d^4\sigma}{dE' d\Omega' d\theta_\pi} = 2\pi\Gamma_{em} \frac{\alpha}{16\pi W^2} \frac{k_\pi}{q} \left(\frac{H_{11} + H_{22}}{2} + \epsilon \frac{Q^2}{q^2} H_{00} \right). \quad (9)$$

$$\Gamma_{em} = \frac{\alpha}{2\pi^2} \frac{E'}{E} \frac{1}{Q^2} \frac{1}{1-\epsilon} k_\gamma^{LAB} \quad (10)$$

$$\epsilon = \left[1 + 2 \frac{q_{LAB}^2}{Q^2} \tan^2\left(\frac{\theta_l}{2}\right) \right]^{-1} \quad (11)$$

Cross Section and Multipole Decomposition

Hadron tensor elements in terms of multipoles:

$$\int d\Omega_\pi \frac{H^{11} + H^{22}}{2} = 2\pi \sum_{l=0} (l+1)^2 \left[(|E_{l+}|^2 + |M_{(l+1)-}|^2) + l(|M_{l+}|^2 + |E_{(l+1)-}|^2) \right], \quad (12)$$

$$\int d\Omega_\pi \frac{1}{2} H^{00} = 4\pi \sum_{l=0} (l+1)^3 (|S_{l+}|^2 + |S_{(l+1)-}|^2) \quad (13)$$

Meson Couplings

